

A Hierarchical Triple Star System in M4

Frederic A. Rasio

Department of Physics, MIT, Cambridge, MA 02139, USA

Abstract. The radio millisecond pulsar PSR B1620–26 is part of an extraordinary triple star system in the globular cluster M4. The inner companion to the neutron star is thought to be a white dwarf of mass $m_1 \simeq 0.3 M_\odot$ in an orbit of period $\simeq 0.5$ yr. The nature and orbital characteristics of the second, more distant companion, have remained a mystery for many years. A theoretical analysis of the latest available radio pulsar timing data is presented here, allowing us to determine approximately the mass and orbital parameters of the second companion. Remarkably, the current best-fit parameters correspond to a second companion of *planetary mass*, with $m_2 \sin i_2 \simeq 7 \times 10^{-3} M_\odot$, in an orbit of eccentricity $e_2 \simeq 0.45$ and with a large semimajor axis $a_2 \simeq 60$ AU. The short dynamical lifetime of this very wide triple in M4 suggests that large numbers of such planets must be present in globular clusters. We also address the question of the anomalously high eccentricity of the inner binary pulsar. While this eccentricity could have been induced during the same dynamical interaction that created the triple, we find that it could also naturally arise from long-term secular perturbation effects in the triple, combining the general relativistic precession of the inner orbit with the Newtonian gravitational perturbation by the outer planet.

1. Introduction

PSR B1620–26 is a unique millisecond radio pulsar. The pulsar is a member of a hierarchical triple system located in or near the core of the globular cluster M4. It is the only radio pulsar known in a triple system, and the only triple system known in any globular cluster. The inner binary of the triple contains the $\simeq 1.4 M_\odot$ neutron star with a $\simeq 0.3 M_\odot$ white-dwarf companion in a 191-day orbit (Lyne *et al.* 1988; McKenna & Lyne 1988). The triple nature of the system was first proposed by Backer (1993) in order to explain the unusually high residual second and third pulse frequency derivatives left over after subtracting a standard Keplerian model for the pulsar binary.

The pulsar has now been timed for 12 years since its discovery (Thorsett, Arzoumanian, & Taylor 1993; Backer, Foster, & Sallmen 1993; Backer & Thorsett 1995; Arzoumanian *et al.* 1996; Thorsett *et al.* 1999). These observations have not only confirmed the triple nature of the system, but they have also provided constraints on the mass and orbital parameters of the second companion. Earlier calculations using three pulse frequency derivatives suggested that the mass of the second companion could be anywhere between $\sim 10^{-3} - 1 M_\odot$, with corre-

sponding orbital periods in the range $\sim 10^2 - 10^3$ yr (Michel 1994; Rasio 1994; Sigurdsson 1995). More recent calculations using four frequency derivatives and preliminary measurements of the orbital perturbations of the inner binary further constrained the mass of the second companion, and suggested that it is most likely a giant planet or a brown dwarf of mass $\sim 0.01 M_\odot$ at a distance ~ 50 AU from the pulsar binary (Arzoumanian *et al.* 1996; Joshi & Rasio 1997, hereafter JR97). In §2 below we summarize our results from the latest theoretical analysis of the pulsar timing data (Ford *et al.* 2000; hereafter FJRZ), including the most recent observations of Thorsett *et al.* (1999; hereafter TACL). The data now include measurements of five pulse frequency derivatives, as well as improved measurements and constraints on various orbital perturbation effects in the triple.

Previous optical observations by Bailyn *et al.* (1994) and Shearer *et al.* (1996) using ground-based images of M4 had identified a possible optical counterpart for the pulsar, consistent with a $\sim 0.5 M_\odot$ main-sequence star, thus contradicting the theoretical results, which suggest a much lower-mass companion. However, it also seemed possible that the object could be a blend of unresolved fainter stars, if not a chance superposition. Later HST WFPC2 observations of the same region by Bailyn (private communication) have resolved the uncertainty. The much higher resolution ($\sim 0.1''$) HST image shows no optical counterpart at the pulsar position, down to a magnitude of $V \simeq 23$, therefore eliminating the presence of any main-sequence star in the system.

PSR B1620–26 is not the first millisecond pulsar system in which a planet (or brown dwarf) has been detected. The first one, PSR B1257+12, is a single millisecond pulsar with three clearly detected inner planets (all within 1 AU) of terrestrial masses in circular orbits around the neutron star (Wolszczan 1994). Preliminary evidence for at least one giant planet orbiting at a much larger distance from the neutron star has also been reported (Wolszczan 1996; JR97). In PSR B1257+12 it is likely that the planets were formed in orbit around the neutron star, perhaps out of a disk of debris left behind following the complete evaporation of a previous binary companion (see, e.g., Podsiadlowski 1995). Such an evaporation process has been observed in several eclipsing binary millisecond pulsars (e.g., Nice *et al.* 2000), where the companion masses have been reduced to $\sim 0.01 M_\odot$ by ablation. These companions used to be ordinary white dwarfs and, although their masses are now quite low, they cannot be properly called either planets or brown dwarfs (Rasio, Pfahl, & Rappaport 2000).

In PSR B1620–26, the hierarchical triple configuration of the system and its location near the core of a dense globular cluster suggest that the second companion was acquired by the pulsar following a dynamical interaction with another object (Rasio, McMillan & Hut 1995; Sigurdsson 1993, 1995; FJRZ). This object could have been a primordial binary with a low-mass brown-dwarf component, or a main-sequence star with a planetary system containing at least one massive giant planet. Indeed the possibility of detecting “scavenged” planets around millisecond pulsars in globular clusters was discussed by Sigurdsson (1992) even before the triple nature of PSR B1620–26 was discovered. Several versions of such a dynamical formation scenario are possible for the triple system, all involving dynamical exchange interactions between binaries in the core of M4. In the most likely scenario, studied in detail by FJRZ, a pre-existing

binary millisecond pulsar has a dynamical interaction with a wide star–planet system, which leaves the planet bound to the binary pulsar while the star is ejected. From numerical scattering experiments we found that the probability of retaining the planet, although smaller than the probability of retaining the star, is always significant, with a branching ratio $\simeq 10\% - 30\%$ for encounters with pericenter distances $r_p/a_i \simeq 0.2 - 1$, where $a_i \sim 50$ AU is the typical initial star–planet separation. All the observed parameters of the triple system are consistent with such a formation scenario, which also allows the age of the millisecond pulsar (most likely $\gtrsim 10^9$ yr) to be much larger than the lifetime of the triple (as short as $\sim 10^7$ yr if it resides in the core of the cluster).

Objects with masses $\sim 0.001 - 0.01 M_\odot$ have recently been detected around many nearby solar-like stars in Doppler searches for extrasolar planets (see Marcy & Butler 1998 for a review). In several cases (e.g., *v* And), more than one object have been detected in the same system, clearly establishing that they are members of a planetary system rather than a very low-mass stellar (brown dwarf) binary companion. For the second companion of PSR B1620–26, of mass $\sim 0.01 M_\odot$, current observations and theoretical modeling do not make it possible to determine whether the object was originally formed as part of a planetary system, or as a brown dwarf. In this paper, we will simply follow our prejudice, and henceforth will refer to the object as “the planet.”

One aspect of the system that remains unexplained, and can perhaps provide constraints on its formation and dynamical evolution, is the unusually high eccentricity $e_1 = 0.025$ of the inner binary. This is much larger than one would expect for a binary millisecond pulsar formed through the standard process of pulsar recycling by accretion from a red-giant companion. During the mass accretion phase, tidal circularization of the orbit through turbulent viscous dissipation in the red-giant envelope should have brought the eccentricity down to $\lesssim 10^{-4}$ (Phinney 1992). At the same time, however, the measured value may appear too small for a dynamically induced eccentricity. Indeed, for an initially circular binary, the eccentricity induced by a dynamical interaction with another star is an extremely steep function of the distance of closest approach (Rasio & Hoggie 1995). Therefore a “typical” interaction would be expected either to leave the eccentricity unchanged, or to increase it to a value of order unity (including the possibility of disrupting the binary).

Secular perturbations in the triple system can also lead to an increase in the eccentricity of the inner binary. A previous analysis assuming nearly coplanar orbits suggested that, starting from a circular inner orbit, an eccentricity as large as 0.025 could only be induced by the perturbation from a stellar-mass second companion (Rasio 1994), which is now ruled out. For large relative inclinations, however, it is known that the eccentricity perturbations can in principle be considerably larger (Kozai 1962; see Ford, Kozinsky & Rasio 2000, hereafter FKR, for a recent treatment). In addition, the Newtonian secular perturbations due to the tidal field of the second companion can combine nonlinearly with other perturbation effects, such as the general relativistic precession of the inner orbit, to produce enhanced eccentricity perturbations (see FKR and §3 below).

2. Analysis of the Pulsar Timing Data

2.1. Pulse Frequency Derivatives

The standard method of fitting a Keplerian orbit to timing residuals cannot be used when the pulsar timing data cover only a small fraction of the orbital period (but see TACL for an attempt at fitting two Keplerian orbits to the PSR B1620–26 timing data). For PSR B1620–26, the duration of the observations ($\simeq 10$ yr) is short compared to the likely orbital period of the second companion, which is $\gtrsim 100$ yr. In this case, pulse frequency derivatives (coefficients in a Taylor expansion of the pulse frequency around a reference epoch) can be derived to characterize the shape of the timing residuals (after subtraction of a Keplerian model for the inner binary). It is easy to show that from *five* well-measured and dynamically-induced frequency derivatives one can obtain a complete solution for the orbital parameters and mass of the companion, up to the usual inclination factor (JR97).

JR97 used the first four time derivatives of the pulse frequency to solve for a one-parameter family of solutions for the orbital parameters and mass of the second companion. The detection of the fourth derivative, which was marginal at the time, has now been confirmed (TACL). In addition, we now also have a preliminary measurement of the fifth derivative. This allows us in principle to obtain a unique solution, but the measurement uncertainty on the fifth derivative is very large, giving us correspondingly large uncertainties on the theoretically derived parameters of the system. Equations and details on the method of solution are presented in JR97, and will not be repeated here.

Our new solution is based on the latest available values of the pulse frequency derivatives, obtained by TACL for the epoch MJD 2448725.5:

$$\begin{aligned}
 \text{Spin Period } P &= 11.0757509142025(18) \text{ ms} \\
 \text{Spin frequency } f &= 90.287332005426(14) \text{ s}^{-1} \\
 \dot{f} &= -5.4693(3) \times 10^{-15} \text{ s}^{-2} \\
 \ddot{f} &= 1.9283(14) \times 10^{-23} \text{ s}^{-3} \\
 \dddot{f} &= 6.39(25) \times 10^{-33} \text{ s}^{-4} \\
 f^{(4)} &= -2.1(2) \times 10^{-40} \text{ s}^{-5} \\
 f^{(5)} &= 3(3) \times 10^{-49} \text{ s}^{-6}
 \end{aligned}$$

Here the number in parenthesis is a conservative estimate of the formal 1σ error on the measured best-fit value, taking into account the correlations between parameters (see TACL for details). It should be noted that the best-fit value for the fourth derivative quoted earlier by Arzoumanian *et al.* (1996) and used in JR97, $f^{(4)} = -2.1(6) \times 10^{-40} \text{ s}^{-5}$, has not changed, while the estimated 1σ error has decreased by a factor of three. This gives us confidence that the new measurement of $f^{(5)}$, although preliminary, will not change significantly over the next few years as more timing data become available.

Since the orbital period of the second companion is much longer than that of the inner binary, we treat the inner binary as a single object. Keeping the same notation as in JR97, we let $m_1 = m_{\text{NS}} + m_c$ be the mass of the inner binary pulsar, with m_{NS} the mass of the neutron star and m_c the mass of the (inner) companion, and we denote by m_2 the mass of the second companion. The

orbital parameters are the longitude λ_2 at epoch (measured from pericenter), the longitude of pericenter ω_2 (measured from the ascending node), the eccentricity e_2 , semimajor axis a_2 , and inclination i_2 (such that $\sin i_2 = 1$ for an orbit seen edge-on). They all refer to the orbit of the second companion with respect to the center of mass of the system (the entire triple). A subscript 1 for the orbital elements refers to the orbit of the inner binary. We assume that $m_{\text{NS}} = 1.35 M_\odot$, giving $m_c \sin i_1 = 0.3 M_\odot$, where i_1 is the inclination of the inner binary (Thorsett *et al.* 1993), and we take $\sin i_1 = 1$ for the analysis presented in this section since our results depend only very weakly on the inner companion mass.

The observed value of \dot{f} is in general determined by a combination of the intrinsic spin-down of the pulsar and the acceleration due to the second companion. However, in this case, the observed value of \dot{f} has changed from $-8.1 \times 10^{-15} \text{s}^{-2}$ to $-5.4 \times 10^{-15} \text{s}^{-2}$ over 11 years (TACL). Since the intrinsic spin-down rate is essentially constant, this large observed rate of change indicates that the observed \dot{f} is almost entirely acceleration-induced. Similarly, the observed value of \ddot{f} is at least an order of magnitude larger than the estimate of \ddot{f} from intrinsic timing noise, which is usually not measurable for old millisecond pulsars (see Arzoumanian *et al.* 1994, TACL, and JR97). Intrinsic contributions to the higher derivatives should also be completely negligible for millisecond pulsars. Hence, in our analysis, we assume that all observed frequency derivatives are dynamically induced, reflecting the presence of the second companion.

Figure 1 illustrates our latest one-parameter family of solutions, obtained using the updated values of the first four pulse frequency derivatives. There are no significant differences compared to the solution obtained previously in JR97. The vertical solid line indicates the unique solution obtained by including the fifth derivative. It corresponds to a second companion mass $m_2 \sin i_2 = 7.0 \times 10^{-3} M_\odot$, eccentricity $e_2 = 0.45$, and semimajor axis $a_2 = 57 \text{ AU}$. For a total system mass $m_1 + m_2 = 1.65 M_\odot$ this gives an outer orbital period $P_2 = 308 \text{ yr}$.

It is extremely reassuring to see that the new measurement of $f^{(5)}$ is consistent with the family of solutions obtained previously on the basis of the first four derivatives. The implication is that the signs and magnitudes of these five independently measured quantities are all consistent with the basic interpretation of the data in terms of a second companion orbiting the inner binary pulsar in a Keplerian orbit. For comparison, the two vertical dashed lines in Figure 1 indicate the change in the solution obtained by decreasing the value of $f^{(5)}$ by a factor of 1.5 (right), or increasing it by a factor of 1.5 (left). Note that lower values of $f^{(5)}$ give higher values for m_2 . If we vary the value of $f^{(5)}$ within its entire 1σ error bar, all solutions are allowed, except for the extremely low-mass solutions with $m_2 \sin i_2 \lesssim 0.002 M_\odot$. In particular, the present 1σ error on $f^{(5)}$ does not strictly rule out a hyperbolic orbit ($e_2 > 1$) for m_2 . However, it is still possible to derive a strict upper limit on m_2 by considering hyperbolic solutions and requiring that the relative velocity at infinity of the perturber be less than the escape speed from the cluster core. Indeed, for $m_2 \sin i_2 > 0.055 M_\odot$, FJRZ find that the relative velocity at infinity would exceed the escape speed from the cluster core ($\simeq 12 \text{ km s}^{-1}$; see Peterson *et al.* 1995). A strict lower limit on the mass, $m_2 \gtrsim 2 \times 10^{-4} M_\odot$, can also be set by requiring that the orbital period of the second companion be longer than the duration of the timing observations

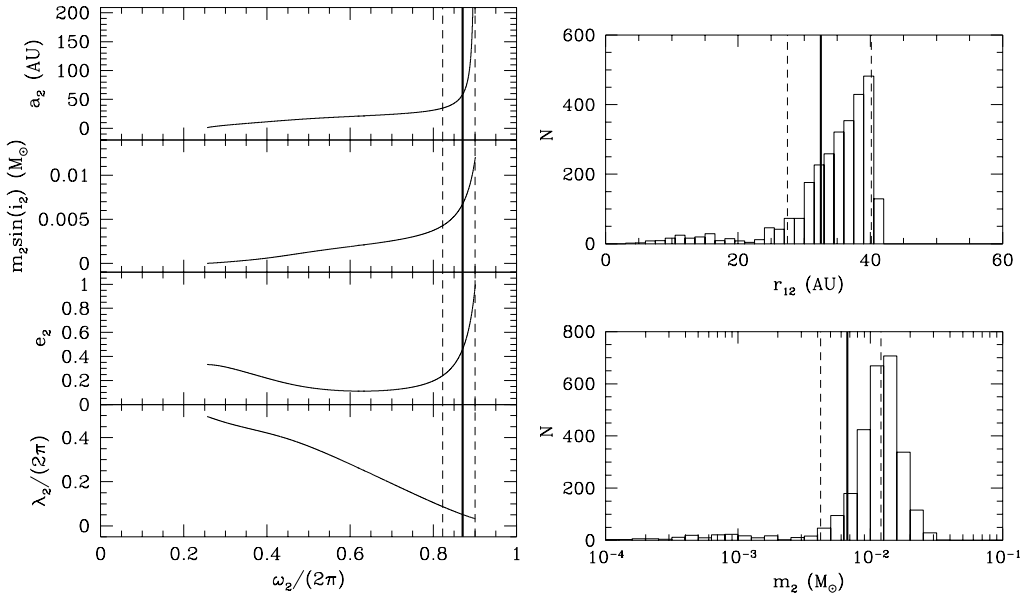


Figure 1. Allowed values of the semimajor axis a_2 , mass m_2 , eccentricity e_2 , longitude at epoch λ_2 , and longitude of pericenter ω_2 for the second companion of PSR B1620–26, using the latest available values for four pulse frequency derivatives (left). On the right, we show the number of accepted realizations (N) of the triple for different values of m_2 and the corresponding distance r_{12} of the second companion from the inner binary in our Monte Carlo simulations. Accepted realizations are those leading to short-term orbital perturbation effects consistent with the current observations. The vertical solid line indicates the complete solution obtained by including the preliminary value of the fifth derivative. The two dashed lines indicate the solutions obtained by decreasing or increasing the value of $f^{(5)}$ by a factor of 1.5.

(about 10 yr). Note that all solutions then give dynamically stable triples, even at the low-mass, short-period limit (Eggleton & Kiseleva 1995; JR97).

2.2. Orbital Perturbations

Additional constraints and consistency checks on the model can be obtained by considering the perturbations of the orbital elements of the inner binary caused by the presence of the second companion. These include a precession of the pericenter, as well as short-term linear drifts in the inclination and eccentricity. The drift in inclination can be detected through a change in the projected semimajor axis of the pulsar. The semimajor axis itself is not expected to be perturbed significantly by a low-mass second companion (Sigurdsson 1995).

The latest measurements, obtained by adding a linear drift term to each orbital element in the Keplerian fit for the inner binary (TACL) give:

$$\begin{aligned}\dot{\omega}_1 &= -5(8) \times 10^{-5} \text{ deg yr}^{-1}, \\ \dot{e}_1 &= 0.2(1.1) \times 10^{-15} \text{ s}^{-1}, \\ \dot{x}_p &= -6.7(3) \times 10^{-13},\end{aligned}$$

where $x_p = a_p \sin i_1$ is the projected semimajor axis of the pulsar. Note that only \dot{x}_p is clearly detected, while the other two measurements only provide upper limits.

We have used these measurements in FJRZ to constrain the system by requiring that all our solutions be consistent with these secular perturbations. Specifically, we perform Monte Carlo simulations, constructing a large number of random realizations of the triple system in 3D, and accepting or rejecting them on the basis of compatibility with the measured orbital perturbations (see JR97 for details). The eccentricity of the outer orbit is selected randomly assuming a thermal distribution, and the other orbital parameters are then calculated from the standard solutions obtained in §2.1. The unknown inclination angles i_1 and i_2 are generated assuming random orientations of the orbital planes, and the two position angles of the second companion are determined using i_1 , i_2 , ω_2 , λ_2 , and an additional undetermined angle α , which (along with i_1 and i_2) describes the relative orientation of the two orbital planes. The perturbations are calculated analytically for each realization of the system, assuming a fixed position of the second companion. The perturbation equations are given in Rasio (1994) and JR97.

Figure 1 (right panel) shows the resulting probability distributions for the mass m_2 and the current separation (at epoch) r_{12} of the second companion. The Monte Carlo trials were performed using only our standard solution based on four pulse frequency derivatives, since the fifth derivative is still only marginally detected. The solid lines indicate the values given by the preliminary measurement of $f^{(5)}$ and assuming $\sin i_2 = 1$. The most probable value of $m_2 \simeq 0.01 M_\odot$ is consistent with the range of values obtained from the complete solution using the fifth derivative. We have also calculated the probability distribution of $f^{(5)}$ predicted by our Monte Carlo simulations, and found that it is consistent with the preliminary measurement, providing yet another independent self-consistency check on our model.

3. Secular Eccentricity Perturbations

We now examine the possibility that the inner binary eccentricity was induced by the secular gravitational perturbation of the second companion. In the hierarchical three-body problem, analytic expressions for the maximum induced eccentricity and the period of long-term eccentricity oscillations are available in certain regimes, depending on the eccentricities and relative inclination of the orbits.

3.1. Planetary Regime

For orbits with small eccentricities and a small relative inclination ($i \lesssim 40^\circ$), the classical solution for the long-term secular evolution of eccentricities and longitudes of pericenters can be written in terms of an eigenvalue and eigenvector formulation (e.g., Murray & Dermott 2000; see Rasio 1995 for simplified expressions in various limits). This classical solution is valid to all orders in the ratio of semimajor axes. The eccentricities oscillate as angular momentum is transferred between the two orbits. The precession of the orbits (libration or circulation) is coupled to the eccentricity oscillations, but the relative inclination remains ap-

proximately constant. In this regime, it can be shown that a stellar-mass second companion would be necessary to induce the observed eccentricity in the inner binary (Rasio 1994; 1995). Such a large mass for the third body has been ruled out by recent timing data (see §2), implying that secular perturbations from a third body in a nearly coplanar and circular orbit does not explain the observed inner eccentricity.

Sigurdsson (1995) has suggested that it may be possible for the secular perturbations to grow further because of random distant interactions of the triple with other cluster stars at distances ~ 100 AU, which would perturb the long-term phase relation between the inner and outer orbits, allowing the inner eccentricity to “random walk” up to a much larger value. However, the current most probable solution from the timing data requires the second companion to be in a very wide orbit (separation $\gtrsim 40$ AU), giving it a very short lifetime in the cluster, and leaving it extremely vulnerable to disruption by such repeated weak encounters (see JR97 for a more detailed discussion).

3.2. High-Inclination Regime

For a triple system formed through a dynamical interaction, there is no reason to assume that the relative inclination of the two orbits should be small. When the relative inclination of the two orbital planes is $\gtrsim 40^\circ$, a different regime of secular perturbations is encountered. This regime has been studied in the past using the quadrupole approximation (Kozai 1962; see Holman, Touma, & Tremaine 1997 for a recent discussion). Here the relative inclination i of the two orbits and the inner eccentricity e_1 are coupled by the integral of motion $\Theta = (1 - e_1^2) \cos^2 i$ (Kozai’s integral). Thus, the amplitude of the eccentricity oscillations is determined by the relative inclination. It can be shown that large-amplitude eccentricity oscillations are possible only when $\Theta < 3/5$ (Holman *et al.* 1997). For an initial eccentricity $e_1 \simeq 0$ and initial inclination i_0 this implies $i_0 > \cos^{-1} \sqrt{3/5} \simeq 40^\circ$ and the maximum eccentricity is then given by $e_{1\max} = [1 - (5/3) \cos^2 i_0]^{1/2}$, which approaches unity for relative inclinations approaching 90° . For a sufficiently large relative inclination, this suggests that it should always be possible to induce an arbitrarily large eccentricity in the inner binary, and that this could provide an explanation for the anomalously high eccentricity of the binary pulsar in the PSR B1620–26 system (Rasio, Ford, & Kozinsky 1997). However, there are two additional conditions that must be satisfied for this explanation to hold.

First, the timescale for reaching a high eccentricity must be shorter than the lifetime of the system. Although the masses, initial eccentricities, and ratio of semimajor axes do not affect the maximum inner eccentricity, they do affect the period of the eccentricity oscillations (see Holman *et al.* 1997; Mazeh *et al.* 1996). The inner longitude of periastron precesses with this period, which can be quite long, sometimes exceeding the lifetime of the system in the cluster. The masses also affect the period, but they decrease the amplitude of the eccentricity oscillations only when the mass ratio of the inner binary approaches unity (FKR). In Figure 2 we compare the period of the eccentricity oscillations to the lifetime of the triple in M4. It is clear that for most solutions the timescale to reach a large eccentricity exceeds the lifetime of the triple. The only possible exceptions are for very low-mass planets ($m_2 \lesssim 0.002 M_\odot$) and with the triple

residing far outside the cluster core. These cannot be excluded, but are certainly not favored by the observations (see §2).

The second problem is that other sources of perturbations may become significant over these long timescales. In particular, for an inner binary containing compact objects, general relativistic effects can become important. This turns out to play a crucial role for the PSR B1620–26 system, and we address this question in detail in the next section.

3.3. General Relativistic Effects

Additional perturbations that affect the longitude of periastron can indirectly change the evolution of the eccentricity of the inner binary in a hierarchical triple. For example, tidally- or rotationally-induced quadrupolar distortions, as well as general relativity, can cause a significant precession of the inner orbit for a sufficiently compact binary. If this additional precession is much slower than the precession due to the secular perturbations, then the eccentricity oscillations are not significantly affected. However, if the additional precession is faster than the secular perturbations, then eccentricity oscillations are severely damped (see, e.g., Holman *et al.* 1997). In addition, if the two precession periods are comparable, then a type of resonance can occur that leads to a significant increase in the eccentricity perturbation (FKR).

Figure 2 compares the various precession periods for PSR B1620-26 as a function of the second companion mass m_2 for the entire one-parameter family of standard solutions constructed in §2. The precession period $P_{\text{High } i}$ for high-inclinations was calculated using the approximate analytic expression given by Holman *et al.* (1997, eq. 3), while $P_{\text{Low } i}$ is from the classical solution (§3.1). The general relativistic precession period for the inner binary, P_{GR} , is also shown. Note that, although we have labeled the plot assuming $\sin i_2 = 1$, only $P_{\text{Low } i}$ has an explicit dependence on m_2 (and it is calculated here for $\sin i_2 = 1$).

For nearly all solutions we find that the general relativistic precession is *faster* than the precession due to the Newtonian secular perturbations. The only exceptions are for low-mass second companions ($m_2 \lesssim 0.005 M_\odot$) in low-inclination orbits. However, we have already mentioned above (§3.1) that in this case the maximum induced eccentricity could not reach the present observed value. Most remarkably, however, we also see from Figure 2 that, for the most probable solution (based on the current measured value of $f^{(5)}$ and indicated by the vertical solid line in the figure), the two precession periods are *nearly equal* for a low-inclination system. This suggests that resonant effects may play an important role in this system, a possibility that we have explored in detail using numerical integrations. We describe the numerical results in the next section.

3.4. Numerical Integrations of the Secular Evolution Equations

If the quadrupole approximation used for the high-inclination regime is extended to octupole order, the resulting secular perturbation equations approximate very well the long-term dynamical evolution of hierarchical triple systems for a wide range of masses, eccentricities, and inclinations (FKR; Krymowski & Mazeh 1999). We have used the octupole-level secular perturbation equations derived by FKR to study the long-term eccentricity evolution of the PSR B1620–26 triple. We integrate the equations using the variables $e_1 \sin \omega_1$,

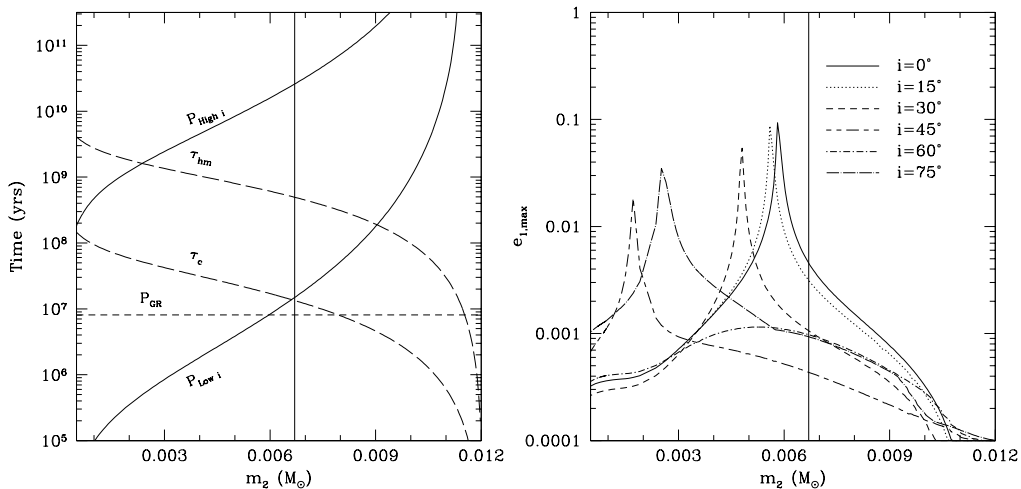


Figure 2. Comparison of the various secular precession timescales in the PSR B1620–26 triple, as a function of the mass of the second companion in the standard solution of §2 (left). Also shown for comparison is the lifetime of the triple, both in the cluster core (τ_c) and at the half-mass radius (τ_{hm}). On the right, we show the maximum eccentricity of the binary pulsar induced by secular perturbations in the triple (including the Newtonian perturbation by the second companion, and the general relativistic precession of the inner orbit), as a function of the mass of the second companion in the one-parameter family of solutions from §2. Note the clear resonant interaction between the Newtonian and relativistic perturbations.

$e_1 \cos \omega_1$, $e_2 \sin \omega_2$, and $e_2 \cos \omega_2$, where ω_1 and ω_2 are the longitudes of pericenters. This avoids numerical problems for nearly circular orbits, and also allows us to incorporate easily the first-order post-Newtonian correction into our integrator, which is based on the Burlish-Stoer method. We assume that the present inner eccentricity is due entirely to the secular perturbations and that the initial eccentricity of the binary pulsar was much smaller than its present value. In addition, we restrict our attention to the standard one-parameter family of solutions constructed in §2.1. From the numerical integrations we can then determine the maximum induced eccentricity.

In Figure 2 (right panel) we show this maximum induced eccentricity in the inner orbit as a function of the second companion mass for several inclinations. For most inclinations and masses, we see that the maximum induced eccentricity is significantly smaller than the observed value, as expected from the discussion of §3.3. However, for a small but significant range of masses near the most probable value (approximately $0.0055 M_\odot < m_2 < 0.0065 M_\odot$), the induced eccentricity for low-inclination systems can reach values $\gtrsim 0.02$.

As already pointed out in §3.2, the maximum induced eccentricity may also be limited by the lifetime of the triple system. From Figure 2 we see that, near resonance, we expect $P_{\text{Low } i} \simeq P_{\text{GR}} \simeq 10^7$ yr, which is comparable to the lifetime of the triple in the cluster core, and much shorter than the lifetime outside of the core. For solutions near a resonance the inner eccentricity e_1 initially

grows linearly at approximately the same rate as it would without the general relativistic perturbation. However, the period of the eccentricity oscillation can be many times the period of the classical eccentricity oscillations. Although this allows the eccentricity to grow to a larger value, the timescale for this growth can then be longer than the expected lifetime of the triple in the cluster core. For example, with $m_2 = 0.006 M_\odot$ we find that the inner binary reaches an eccentricity of 0.025 after about 1.5 times the expected lifetime of the triple in the core of M4. Thus, even if the system is near resonance, it must probably still be residing somewhat outside the core for the secular eccentricity perturbation to have enough time to grow to the currently observed value.

4. Summary

Our theoretical analysis of the latest timing data for PSR B1620–26 clearly confirms the triple nature of the system. Indeed, the values of all five measured pulse frequency derivatives are consistent with our basic interpretation of a binary pulsar perturbed by the gravitational influence of a more distant object on a bound Keplerian orbit. The results of our Monte-Carlo simulations based on the four well-measured frequency derivatives and preliminary measurements of short-term orbital perturbation effects in the triple are consistent with the complete solution obtained when we include the preliminary measurement of the fifth frequency derivative. This complete solution corresponds to a second companion of mass $m_2 \sin i_2 \simeq 7 \times 10^{-3} M_\odot$ in an orbit of eccentricity $e_2 \simeq 0.45$ and semimajor axis $a_2 \simeq 60$ AU (orbital period $P_2 \simeq 300$ yr). Although the present formal 1σ error on $f^{(5)}$ is large, we do not expect this solution to change significantly as more timing data become available.

It is possible that the dynamical interaction that formed the triple also perturbed the eccentricity of the binary pulsar to the anomalously large value of 0.025 observed today. However, we have shown that, through a subtle interaction between the general relativistic corrections to the binary pulsar’s orbit and the Newtonian gravitational perturbation of the planet, this eccentricity could also have been induced by long-term secular perturbations in the triple after its formation. The interaction arises from the near equality between the general relativistic precession period of the inner orbit and the period of the Newtonian secular perturbations for a low-inclination system. It allows the eccentricity to slowly build up to the presently observed value, on a timescale that can be comparable to the lifetime of the triple in M4.

All dynamical formation scenarios have to confront the problem that the lifetimes of both the current triple and its parent star–planet system are quite short, typically $\sim 10^7 - 10^8$ yr as they approach the cluster core, where the interaction is most likely to occur. Therefore, the detection of a planet in orbit around the PSR B1620–26 binary clearly suggests that large numbers of these wide star–planet systems must exist in globular clusters, since most of them will be destroyed before (or soon after) entering the core, and most planets will not be able to survive long in a wide orbit around any millisecond pulsar system (where they may become detectable through high-precision pulsar timing). Although a star–planet separation $a_i \sim 50$ AU may seem quite large when compared to the orbital radii of all recently detected extrasolar planets (which are all smaller

than a few AU; see Marcy & Butler 1998), one must remember that the current Doppler searches are most sensitive to planets in short-period orbits, and that they could never have detected a low-mass companion with an orbital period $\gg 10$ yr. Similarly, the recent HST search for planetary transits in 47 Tuc by Gilliland *et al.* (2000), which did not detect any planet, was only sensitive to very short orbital periods $\lesssim 10$ d. In addition, it is of course possible that the parent system may have been a primordial binary star with a low-mass, brown dwarf component, rather than a main-sequence star with planets.

Acknowledgments. Many MIT students have contributed significantly to this work, including most recently J. Bostick, E.B. Ford, K.J. Joshi, B. Kozinsky, J. Madic, and B. Zbarsky. This work was supported by NSF Grant AST-9618116 and NASA ATP Grant NAG5-8460, and by a Sloan Research Fellowship.

References

- Arzoumanian, Z., Fruchter, A.S., & Taylor, J.H. 1994, ApJ, 426, L85
- Arzoumanian, Z., Joshi, K.J., Rasio, F.A., & Thorsett, S.E. 1996, in IAU Colloquium 160, Pulsars: Problems and Progress, ASP Conference Series Vol. 105, eds. S. Johnston, *et al.* (San Francisco: ASP), 525
- Arzoumanian, Z., Nice, D.J., Taylor, J.H., & Thorsett, S.E. 1994, ApJ, 422, 621
- Backer, D.C. 1993, in Planets around Pulsars, ASP Conference Series Vol. 36, eds. J.A. Phillips, *et al.* (San Francisco: ASP), 11
- Backer, D.C., Foster, R.S., & Sallmen, S. 1993, Nature, 365, 817
- Backer, D.C., & Thorsett, S.E. 1995, in Millisecond Pulsars: A Decade of Surprise, ASP Conference Series Vol. 72, eds. A.S. Fruchter, *et al.* (San Francisco: ASP), 387
- Bailyn, C.D., Rubinstein, E.P., Girard, T.M., Dinescu, D.I., Rasio, F.A. & Yanny, B. 1994, ApJ, 433, L89
- Cudworth, K.M. & Hansen, R.B. 1993, AJ, 105, 168
- Eggleton, P., & Kiseleva, L. 1995, ApJ, 455, 640
- Ford, E.B., Joshi, K.J., Rasio, F.A., & Zbarsky, B. 2000, ApJ, 528, 336 [FJRZ]
- Ford, E.B., Kozinsky, B., & Rasio, F.A. 2000, ApJ, 535, 385 [FKR]
- Gilliland, R.L., *et al.* 2000, ApJ Letters, in press [astro-ph/0009397]
- Holman, M., Touma, J. & Tremaine, S. 1997, Nature, 386, 254
- Joshi, K.J., & Rasio, F.A. 1997, ApJ, 479, 948; erratum 488, 901. [JR97]
- Kozai, Y., 1962, AJ, 67, 591
- Krymowski, Y., & Mazeh, T. 1999, MNRAS, 304, 720
- Lyne, A.G., *et al.* 1988, Nature, 332, 45
- Marcy, G.W., & Butler, R.P. 1998, ARAA, 36, 57
- Mazeh, T., Krymowski, Y., & Rosenfeld, G. 1996, ApJ, 466, 415
- McKenna, J., & Lyne, A.G. 1988, Nature, 336, 226; erratum, 336, 698
- Michel, F.C. 1994, ApJ, 432, 239
- Murray, C.D., & Dermott, S.F. 2000, Solar System Dynamics (Cambridge University Press)

- Nice, D.J., Arzoumanian, Z., & Thorsett, S.E. 2000, in Pulsar Astronomy – 2000 and Beyond, ASP Conference Series Vol. 202, eds. M. Kramer, *et al.* (San Francisco: ASP), 67
- Peterson, R.C., Rees, R.F., & Cudworth, K.M. 1995, ApJ 443, 124
- Phinney, E.S. 1992, Phil. Trans. R. Soc. Lond., A, 341, 39
- Podsiadlowski, P. 1995, in Millisecond Pulsars: A Decade of Surprise, ASP Conference Series Vol. 72, eds. A.S. Fruchter, *et al.* (San Francisco: ASP), 411
- Rasio, F.A. 1994, ApJ, 427, L107
- Rasio, F.A. 1995, in Millisecond Pulsars: A Decade of Surprise, ASP Conference Series Vol. 72, eds. A.S. Fruchter, *et al.* (ASP, San Francisco), 424
- Rasio, F.A., Ford, E.B., & Kozinsky, B. 1997, AAS Meeting 191, 44.16
- Rasio, F.A., & Heggie, D.C. 1995, ApJ, 445, L133
- Rasio, F.A., McMillan, S., & Hut, P. 1995, ApJ, 438, L33
- Rasio, F.A., Pfahl, E.D., & Rappaport, S. 2000, ApJ, 532, L47
- Shearer, A., *et al.* 1996, ApJ, 473, L115
- Sigurdsson, S. 1992, ApJ, 399, L95
- Sigurdsson, S. 1993, ApJ, 415, L43
- Sigurdsson, S. 1995, ApJ, 452, 323
- Thorsett, S.E., Arzoumanian, Z., & Taylor, J.H. 1993, ApJ, 412, L33
- Thorsett, S.E., Arzoumanian, Z., Camilo, F., & Lyne, A.G. 1999, ApJ, 523, 763 [TACL]
- Wolszczan, A. 1994, Science, 264, 538
- Wolszczan, A. 1996, in IAU Colloquium 160, Pulsars: Problems and Progress, ASP Conference Series Vol. 105, eds. S. Johnston, *et al.* (San Francisco: ASP), 91.